ISSN 1807-1929
Revista Brasileira de Engenharia Agrícola e Ambiental
Brazilian Journal of Agricultural and Environmental Engineering
v.28, n.9, e275829, 2024
Campina Grande, PB – http://www.agriambi.com.br – http://www.scielo.br/rbeaa

DOI: http://dx.doi.org/10.1590/1807-1929/agriambi.v28n9e275829 ORIGINAL ARTICLE

# Fluid dynamic models of ozone application in stored maize[1]

## Modelos fluidodinâmicos de aplicação de ozônio em milho armazenado

Débora B. M. Monteiro[2] & Licinius D. S. de Alcantara[2*]

[1] Research developed at Universidade Federal Rural da Amazônia, Belém, PA, Brazil
[2] Universidade Federal Rural da Amazônia, Belém, PA, Brazil

*HIGHLIGHTS:*

*The results of ozone distribution in the grain mass are affected by modifying the grain distribution model in the container.*
*In a homogeneous grain distribution model, ozone absorption near the container walls is more elevated.*
*In a heterogeneous model, where smaller grains accumulate in the center, ozone absorption near the central axis is greater.*

**ABSTRACT:** In recent years, grain storage in Brazil underwent a 1.5% increase in its available capacity, leading to a high demand for grain treatment in the country. This study aims to evaluate two computational models for grain distribution within stored maize, comparing their ability to predict the effectiveness of ozone application. Specifically, it was investigated whether a heterogeneous model, which accounts for variations in grain density and location, provides results more compatible with experimental observations in the literature. By comparing the predictive capabilities of both models, this study will contribute to developing more effective and targeted strategies for ozone-based pest control in stored grain. In the heterogeneous model, the smaller grains accumulate in the center of the container. The study uses the Stokes-Brinkman model and ozone transport equations in porous media. It was observed that the grain distribution model affects the spatial distribution of ozone concentration inside the container. In the heterogeneous grain distribution model, the region of larger grains presents a lower ozone absorption since supposedly a smaller number of ozone elimination reactions occur on the grain surfaces.

**Key words:** transport of diluted species, porous media, computational fluid dynamics

**RESUMO:** Nos últimos anos, a armazenagem de grãos no Brasil teve um aumento de 1,5% em sua capacidade disponível, levando a uma alta demanda por tratamento de grãos no país. Este estudo tem como objetivo avaliar dois modelos computacionais de distribuição de grãos no milho armazenado, comparando sua capacidade de prever a eficácia da aplicação de ozônio. Especificamente, foi investigado se um modelo heterogêneo, que leva em conta variações na densidade e localização dos grãos, fornece resultados mais compatíveis com observações experimentais na literatura. Ao comparar as capacidades preditivas de ambos os modelos, este estudo contribuirá para o desenvolvimento de estratégias mais eficazes e direcionadas para o controle de pragas com base no ozônio em grãos armazenados. No modelo heterogêneo, os grãos menores acumulam-se no centro do recipiente. O estudo usa o modelo Stokes-Brinkman e as equações de transporte de ozônio em meios porosos. Foi observado que o modelo de distribuição de grãos afeta a distribuição espacial da concentração de ozônio dentro do recipiente. No modelo heterogêneo de distribuição de grãos, a região de grãos maiores apresenta uma menor absorção de ozônio, pois supostamente ocorre um menor número de reações de eliminação de ozônio nas superfícies dos grãos.

**Palavras-chave:** transporte de espécie diluída, meios porosos, fluidodinâmica computacional

• Ref. 275829 – Received 21 Jun, 2023
* Corresponding author - E-mail: licinius@ufra.edu.br
• Accepted 14 Apr, 2024 • Published 06 May, 2024
Editors: Lauriane Almeida dos Anjos Soares & Carlos Alberto Vieira de Azevedo

## Introduction

Brazil, which produced 183.3 million tons in the second half of 2021 (IBGE, 2021), faces challenges storing vast quantities of grain. The grains (soy, wheat, rice, coffee) are susceptible to quality loss during storage due to numerous factors (Błaszkiewicz et al., 2023). Grains comprise carbohydrates, nutrients, protein, and fat in varying proportions, and physically, they exhibit distinct sizes, shapes, colors, and hardness (Serna-Saldívar, 2010). Tropical, hot, and humid conditions favor the development of mycotoxigenic fungi and place Brazil at high risk of mycotoxin contamination (Rocha et al., 2020). Integrated food production, transport, and storage are crucial in modern agriculture, which aims to minimize losses and ensure quality (Dayong et al., 2019). Grain losses due to biological, physical, and chemical contaminants reach 10% of national production (SNAR, 2018).

In minimizing losses, safe and efficient fumigation methods are crucial (Dias et al., 2020; Reddy et al., 2021). Ozone is applied in stored grains via forced flow (Incropera & Dewitt, 2003) and is effective against insects and fungi (Lemic et al., 2019; Afsah-Hejri et al., 2020) but current methods use very high concentrations (Baskakov et al., 2022).

Established computational fluid dynamics (CFD) modeling techniques are used in various agricultural applications (Silva et al., 2020; Marcato et al., 2021; Babadi et al., 2022). These allow researchers to simulate realistic storage conditions (Bournet & Rojano, 2022; Binelo et al., 2019). Mathematical and computational modeling techniques are fundamental tools for improving the design of these storage processes (Mellmann et al., 2011).

By comparing two models for grain distribution, this study aims to see if a heterogeneous model better aligns with existing data and reflects real storage conditions more appropriately. The grain mass is modeled as a porous medium using the Stokes-Brinkman model to account for the impact of grain arrangement on airflow.

## Material and Methods

In this study, the simulations consider an experiment described in the literature by Kells et al. (2001), where the injection of ozone gas in a container with stored maize was analyzed. The computational models were developed at the Universidade Federal Rural da Amazônia (UFRA). This study presented a two-dimensional adaptation of the mass transport problem reported in the literature, considering maize as a porous environment. The developed models adopt CFD modeling to simulate the kinetics of air inside the container. The physical models also consider the transport and elimination of ozone and the convergence of diluted ozone concentrations. The simulations consider a stationary regime, where the convergence of ozone concentration in the stored maize is analyzed.

The results in Figure 1 show the grain container geometry considered in the simulations. Modeling begins with a rectangular inlet highlighted at the top, where ozone gas enters the container. The container height is 3.0 m, and its basis length is 0.57 m. The authors developed two distinct models for spatial grain distribution. In Figure 1A, the grain distribution is homogenous so that the reaction rate coefficient for ozone is constant inside the container, which means that ozone concentration reduces in the same proportion as the air with diluted ozone flows inside it. In Figure 1B, the model assumes that smaller grains accumulate more in the center of the container. This consideration implies that ozone is eliminated more quickly in the center of the container than near its walls, as this elimination depends on the number of surface reactions that occur from the contact of the ozone gas with the grains.

These distinctions in grain distribution, as shown in Figure 1B, aim to make the analysis closer to a real situation, and the results obtained will be discussed in the next section. Environmental factors such as humidity and air impurities affect the performance of ozone generators and the fluid dynamic parameters in the experiments (Kells et al., 2001). The CFD simulations account for moisture- and impurity-free air since it is possible to use a synthetic air input in the ozone generators, which is practically free of these factors, as done by Silva et al. (2019).

Eq. 1, given by the Stokes-Brinkman model, was used to model the airflow in the porous medium formed by the mass of grains; this equation describes a laminar flow in this porous medium when the forces due to viscosity are predominant when compared to the inertial forces. In this case, the stress vector is proportional to the fluid viscosity μ and the infinitesimal strain of the fluid over time (∇u), as shown by the equation below:

$$\tau = \mu\left(\nabla u + \nabla u^{T}\right) \quad (1)$$

where:

τ - stress tensor, N m$^{2}$;

∇u - Jacobian matrix of the velocity field, s$^{-1}$; and,

μ - viscosity of the air, kg m$^{-1}$ s$^{-2}$.

As Krotkiewski et al. (2011) described, this flow has a very small Reynolds number because of its low velocity.

The Stokes-Brinkman equation for a steady state flow, which is derived from Newton's second law, is given by

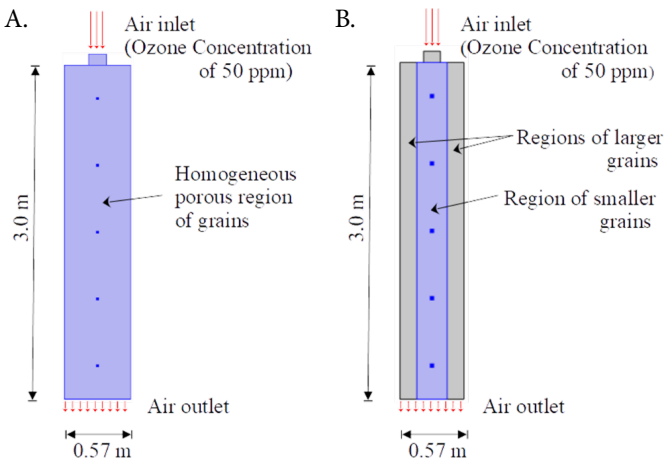


**Figure 1.** Features of the considered models. (A) model considering the homogeneous distribution of grains, and (B) model of regions containing grains of different sizes

$$u + \left(\frac{k}{\mu}\right)\left(\nabla p - \rho g - \mu * \nabla^2 u\right) = 0 \quad (2)$$

where:

u - air velocity vector, m $s^{-1}$;
k - permeability tensor of the porous media, $m^2$;
μ, μ* - viscosity and effective viscosity of the air, kg $m^{-1}$ $s^{-2}$;
p - air pressure, N $m^{-2}$;
ρ - density of the air, kg $m^{-3}$;
g - acceleration of gravity, m $s^{-2}$;
∇p - gradient of air pressure, N $m^{-3}$; and,
$\nabla^2 u$ - Laplacian of velocity, $m^{-1}$ $s^{-1}$.

The equations that model ozone transport in the porous medium are given by

$$\nabla \cdot J + u \cdot \nabla c = R \quad (3)$$

$$J = -D_e \nabla c \quad (4)$$

$$D_e = \varepsilon_p D_F \quad (5)$$

where:

J - diffusive flux vector, mol $m^{-2}$ $s^{-1}$;
u - air velocity vector, m $s^{-1}$;
c - ozone concentration in the fluid, mol $m^{-3}$;
R - reaction rate, mol $m^{-3}$ $s^{-1}$;
∇ · J - divergent of the diffusive flux vector, mol $m^{-3}$ $s^{-1}$;
∇c - gradient of the ozone concentration, mol $m^{-4}$;
$D_e$ - effective diffusion coefficient, $m^2$ $s^{-1}$;
$D_F$ - diffusion coefficient of the fluid, $m^2$ $s^{-1}$; and,
$\varepsilon_p$ - porosity of the medium, dimensionless.

According to Codina (1993), Eq. 3 includes diffusion transport and convection mechanisms. The vector J is related to the mass flux relative to the average mass velocity, which also considers transport due to molecular diffusion and can be calculated from Eq. 4. Eq. 5 refers to saturated porous media and balances mass transport through the porous medium using the porosity $\varepsilon_p$, which is equal to the net volume fraction and varies between 0 and 1.

The right-hand side term of Eq. 3 describes the production or consumption of the species, with R being an expression of the reaction rate that can take into account chemical reactions of production or elimination of the species in the liquid, solid, or gaseous phase. In the problem addressed in this study, the elimination of ozone occurs all over the porous media, which is proportional to the ozone concentration that varies spatially. Therefore, R can be expressed as

$$R = -k \cdot c \quad (6)$$

where:

R - reaction rate, mol $m^{-3}$ $s^{-1}$;
k - reaction rate coefficient for ozone, $s^{-1}$; and,
c - ozone concentration in the fluid, mol $m^{-3}$.

The differential equations that characterize the problem are numerically solved using the finite element method with PARDISO ("Parallel Direct Solver"), as proposed by Schenk et al. (2001). This solver implements an efficient supernodal method, which is a version of Gaussian elimination for large sparse systems of equations (Fialko, 2021). Figure 2 presents the finite element meshes used in the simulation models. These elements are distributed over a total area of 1,725 $m^2$. Each grid element provides local information on air velocity, pressure, and species concentration to enable the numerical calculation of the distribution of these quantities or vectors in space. The data in Table 1 show the parameters used in the mathematical model.

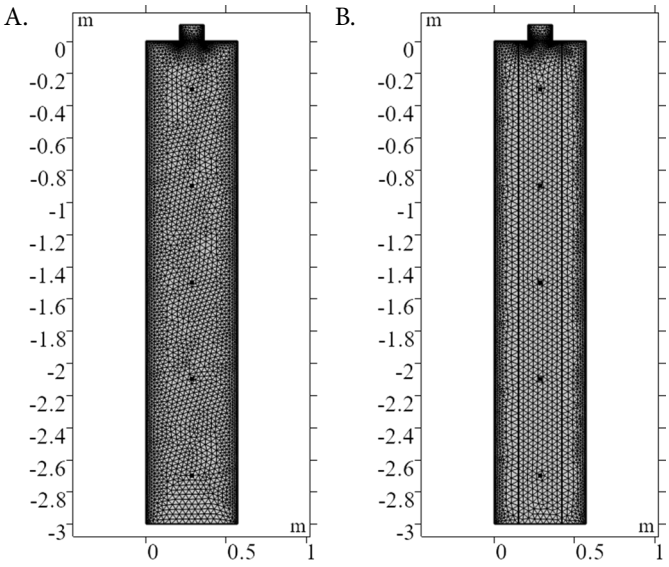


**Figure 2.** Finite element mesh for the simulation models: (A) model considering the homogeneous distribution of grains, containing 6,800 elements, and (B) model of regions with different granularities, containing 5,951 elements

**Table 1.** Physical parameters for the computational fluid dynamics models

| Parameter | Description | Value |
|---|---|---|
| μ | Viscosity of air | $1.825 \times 10^{-5}$ kg $m^{-1}$ $s^{-1}$ |
| $\varepsilon_p$ | Porosity | 0.4 |
| $D_e$ | Effective diffusion coefficient | $5.16 \times 10^{-7}$ $m^2$ $s^{-1}$ |
| $k_1$ | Reaction rate coefficient* | 0.002073 $s^{-1}$ |
| $k_2$ | Reaction rate coefficient** | 0.001382 $s^{-1}$ |
| $p_i$ | Input air pressure (inlet) | 3.3 atm |
| $p_o$ | Output air pressure (outlet) | 1 atm |

* - Used in the homogeneous model and for the region of smaller grains; ** - Used for regions of larger grains

## Results and Discussion

In the simulations, an air pressure of 3.3 atm was assigned to the upper inlet, and the ozone concentration at the inflow was set to 50 ppm. It was considered that at the base of the container, the outlet is under atmospheric pressure.

The results of the distribution of air velocity and ozone concentration for the two models presented in Figure 1 are shown in Figures 3 and 4. Results in Figures 3A and 4A show nearly identical velocity distributions. In both cases, air containing ozone gas enters the container with a velocity of 0.013 m $s^{-1}$ at the inlet. As the flow progresses deeper into the container, the velocity gradually decreases and stabilizes around 0.0036 m $s^{-1}$. There is no observable difference in the

air velocity value in the regions with grains, considering the two models. It is probably due to the airflow characteristics in the porous medium in both cases, where viscous forces are predominant and offer substantial resistance to airflow. Other aspects, such as the quality of the grain, the storage system, and the environmental factors in the storage, may affect the airflow characteristics (Rocha et al., 2020).

However, the differences in ozone concentration at regions close to the wall are notable between the two models (Figures 3B and 4B). In the first model, the maize characteristics are unchangeable inside the container. The second model adopts a heterogeneous grain distribution model, where the region with larger grains presents a lower absorption of ozone since, supposedly, there will be fewer ozone elimination reactions on the surfaces of the grains due to the higher spacing between them in these regions. In both cases, the concentration starts from an input value of 50 ppm, as determined by Kells et al. (2001), and it reduces according to the depth inside the container. However, in the heterogeneous grains model, ozone is eliminated more slowly in regions close to the walls so that, after a given depth, the container starts to present higher ozone concentration levels than in its center. In other words, in the center of the container where the smaller grains have accumulated, the ozone concentration decreases more quickly with depth so that a lower degree of elimination of ozone occurs near the container walls. In the central region, the airflow is exposed to a larger total surface area of the grains, which are closer to each other in this region, and the density of the grains is higher than in those close to the walls.

Now consider the air velocity magnitude along the container depth for two cases: 1) in the center, along the container longitudinal axis, and 2) near the container wall (Figure 5). In the center and along the longitudinal axis, the gas velocity changes faster until it assumes a continuous value stabilizing in 0.0036 m $s^{-1}$ after a depth of 0.5 m in the container. The regions close to the walls are not in the line of sight with the air source. Therefore, the air velocity magnitude starts measuring zero at the top of the container, but it increases with depth due to the incoming airflow lines that diverge from the source to the walls, as shown in Figures 3A and 4A. The results in Figure 5 show if the container were more profound, the velocity near the wall would converge with the velocity value measured at the center at some depth.

Figure 6 displays the steady-state results of ozone concentration over the container depth. The concentration values are computed along two vertical reference lines: one in the center and the other close to the container wall. Note that the ozone gas diffuses and suffers elimination as the air flows deeper inside the container. In Figures 6A and B, the ozone concentration suffers reduction starting from 50 ppm at the top of the central region, where the smaller grains accumulated. Near the walls, where the larger grains remain, the ozone concentration decreases more slowly with depth because, in this region, the rate of ozone elimination is lower. The results in Figure 6B show that from a certain depth, the ozone concentrations near the wall exceed the concentrations measured in the center of the container, which does not occur in Figure 6A. This last result qualitatively agrees with the experimental observations reported by Kells et al. (2001).

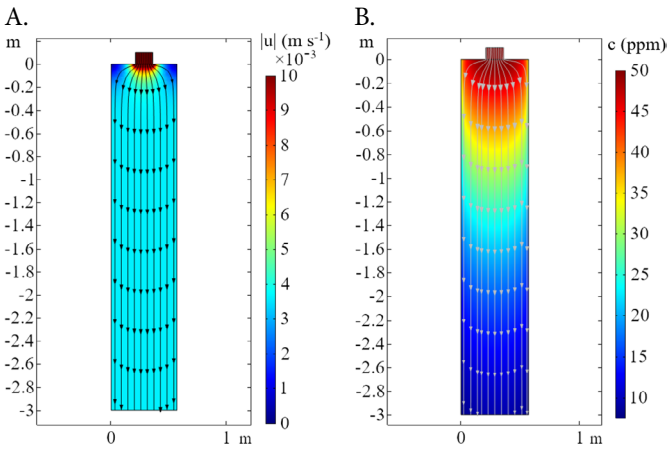


**Figure 3.** Fluid dynamic modeling in spatial distributions for the homogeneous grain model: (A) air velocity, |u| (m $s^{-1}$); (B) ozone concentration, c (ppm)

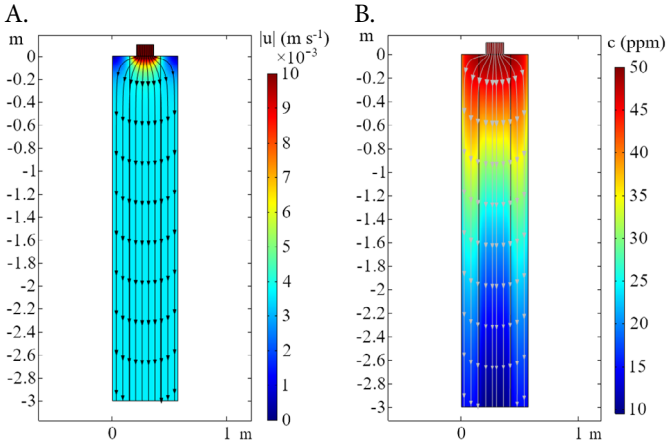


**Figure 4.** Results of fluid dynamic modeling in spatial distributions for the heterogeneous grain model: (A) air velocity, |u| (m $s^{-1}$); (B) ozone concentration, c (ppm)

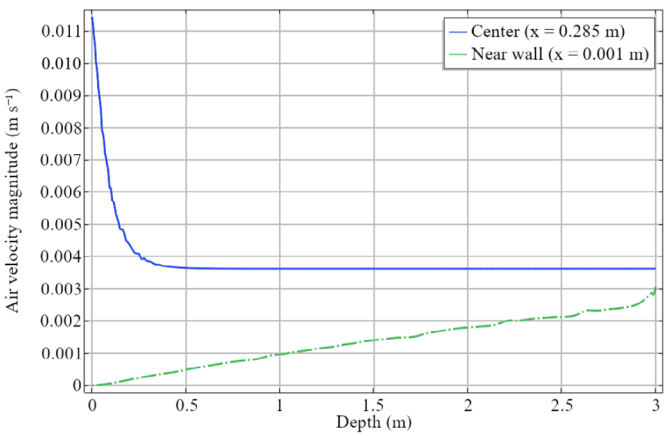


**Figure 5.** Fluid dynamic model for the air velocity magnitude according to the depth in the center of the container and near its wall

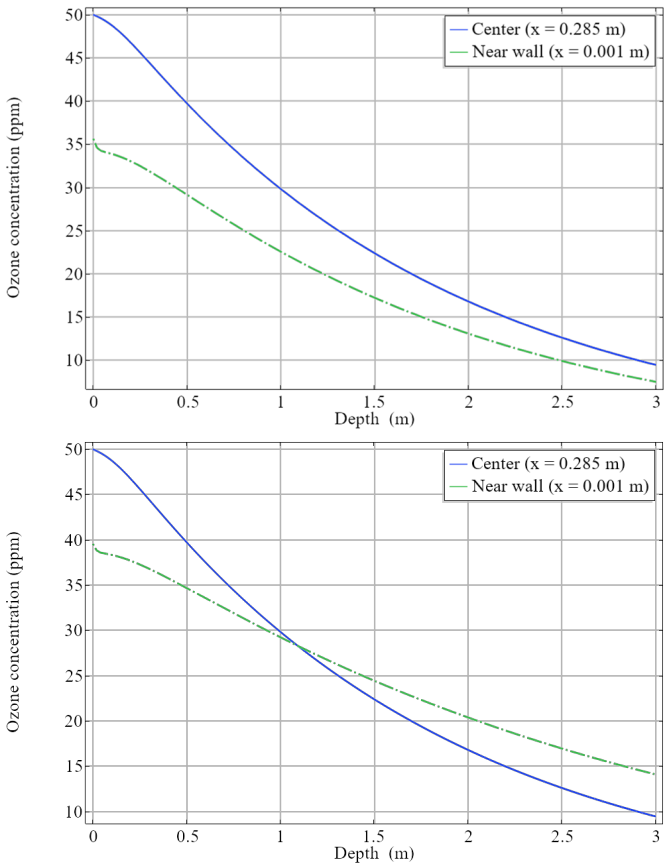


**Figure 6.** Ozone concentration according to the depth in the center and near the container wall: (A) homogeneous grain model; (B) heterogeneous grain model

## Conclusions

1. Changing the grain distribution configuration in the CFD model impacts the way that ozone is distributed and absorbed inside the container.

2. The decision to employ also simulations with both small and large grains arose due to discrepancies observed between the ozone distribution predicted by the uniform-size model and the published experimental data. Therefore, adopting a heterogeneous grain model became necessary to deepen the analysis of the models.

3. The results for the heterogeneous grain distribution model were more qualitatively compatible with aspects described from experimental observations in the literature, in which the ozone concentrations decay slower near the container walls.

**Contribution of authors:** Débora B. M. Monteiro worked on preparing the first version of the manuscript, literature review, research, data acquisition, data analysis, and implementation of the computational models. Licinius D. S. Alcantara acted as a research advisor and worked on the conceptualization of the problem, improvements, corrections to the manuscript, translation into English, literature review, data analysis, and corrections and improvements to the simulation models.

**Supplementary documents:** There are no supplementary sources.

**Conflict of interest:** The authors declare no conflict of interest.

**Financing statement:** This research was partially funded by the Scientific and Technological Initiation Program of PROPED/UFRA through an undergraduate research scholarship awarded for project number PICE474-2021.

## Literature Cited

Afsah-Hejri, L.; Hajeb, P.; Ehsani, R. J. Application of ozone for degradation of mycotoxins in food: A review. Comprehensive Reviews in Food Science and Food Safety, v.19, p.1777-1808, 2020. https://doi.org/10.1111/1541-4337.12594

Babadi, K. A.; Khorasanizadeh, H.; Aghaei, A. CFD modeling of air flow, humidity, $CO_2$ and $NH_3$ distributions in a caged laying hen house with tunnel ventilation system. Computers and Electronics in Agriculture, v.193, e106677, 2022. https://doi.org/10.1016/j.compag.2021.106677

Baskakov, I. V.; Orobinsky, V. I.; Gievsky, A. M.; Gulevsky, V. A.; Chernyshov, A. V. Grain disinfestation with ozone-air mixture. IOP Conference Series: Earth and Environmental Science, v.1043, e012037, 2022. https://doi.org/10.1088/1755-1315/1043/1/012037

Binelo, M. O.; Lima, R. F. de; Khatchatourian, O. A.; Stránský, J. Modelling of the drag force of agricultural seeds applied to the discrete element method. Biosystems Engineering, v.178, p.168-175, 2019. https://doi.org/10.1016/j.biosystemseng.2018.11.013

Błaszkiewicz, J.; Nowakowska-Bogdan, E.; Barabosz, K.; Kulesza, R.; Dresler, E.; Woszczynski, P.; Bilos, L.; Matuszek, D. B.; Szkutnik, K. Effect of green and roasted coffee storage conditions on selected characteristic quality parameters. Scientific Reports, v.13, e6447, 2023. https://doi.org/10.1038/s41598-023-33609-x

Bournet, P. E.; Rojano, F. Advances of Computational Fluid Dynamics (CFD) applications in agricultural building Modelling: Research, Applications and Challenges. Computers and Electronics in Agriculture, v.201, e107277, 2022. https://doi.org/10.1016/j.compag.2022.107277

Codina, R. A discontinuity-capturing crosswind-dissipation for the finite element solution of the convection-diffusion equation. Computer Methods in Applied Mechanics and Engineering, v.110, p.325-342, 1993. https://doi.org/10.1016/0045-7825(93)90213-H

Dayong, N.; Mikhaylov, A.; Bratanovsky, S.; Shaikh, Z. A.; Stepanova, D. Mathematical modeling of the technological processes of catering products production. Journal of Food Process Engineering, v.43, e13340, 2019. https://doi.org/10.1111/jfpe.13340

Dias, T. F. V.; Arcanjo, L. L.; Costa, G. L.; Souza, C. S.; Lima, C. A. R. Controle de pragas e tratamento de grãos armazenados para uso em rações para animais. Research, Society and Development, v.9, e739996964, 2020. https://doi.org/10.33448/rsd-v9i9.6964

Fialko, S. Parallel finite element solver for multi-core computers with shared memory, Computers & Mathematics with Applications, v.94, p.1-14, 2021. https://doi.org/10.1016/j.camwa.2021.04.013

IBGE - Instituto Brasileiro de Geografia e Estatística. Pesquisa de estoques, Rio de Janeiro, p.1-17. 2021. Available on: <https://ftp.ibge.gov.br/Estoque/Pesquisa_de_Estoques_%5Bsemestral%5D/2021_2_semestre/BR_2_semestre2021.pdf> Acessed on: Jun. 2023.

Incropera, F. P.; Dewitt, D. P. Fundamentos da transferência de calor. 5.ed. Rio de Janeiro: Livros Técnico e Científicos, 2003. 698p.

Kells, S. A.; Mason, L. J.; Maier, D. E.; Woloshuk, C. P. Efficacy and fumigation characteristics of ozone in stored maize. Journal of Stored Products Research, v.37, p.371-383, 2001. https://doi.org/10.1016/S0022-474X(00)00040-0

Krotkiewski, M.; Ligaarden, I.; Lie, K.; Schmid, D. On the importance of the Stokes-brinkman equations for computing effective permeability in karst reservoirs. Communications in Computational Physics, v.10, p.1315-1332, 2011. https://doi.org/10.4208/cicp.290610.020211a

Lemic, D.; Jembrek, D.; Bažok, R.; Pajač Živković, I. Ozone Effectiveness on Wheat Weevil Suppression: Preliminary Research. Insects, v.10, e357, 2019. https://doi.org/10.3390/insects10100357

Marcato, A.; Boccardo, G.; Marchisio, D. L. A computational workflow to study particle transport and filtration in porous media: Coupling CFD and deep learning. Chemical Engineering Journal, v.417, e128936, 2021. https://doi.org/10.1016/j.cej.2021.128936

Mellmann, J.; Iroba, K. L.; Metzger, T.; Tsotsas, E., Mészáros, C.; Farkas, I. Moisture content and residence time distributions in mixed-flow grain dryers. Biosystems Engineering, v.109, p.297-307, 2011. https://doi.org/10.1016/j.biosystemseng.2011.04.010

Reddy, S. V. R.; Rao, D. V. S.; Sharma, R.; Preethi, P.; Pandiselvam, R. Role of ozone in post-harvest disinfection and processing of horticultural crops: A review. Ozone: Science & Engineering, v.44, p.127-146, 2021. https://doi.org/10.1080/01919512.2021.1994367

Rocha, M. P.; Taveira, J. H. da S.; Prado, S. M. A.; Ataíde, M. V. Sistema de armazenamento e incidência dos principais fungos produtores de micotoxinas em grãos. Brazilian Journal of Development, v.6, p.50176-50193, 2020. https://doi.org/10.34117/bjdv6n7-608

Schenk, O.; Gärtner, K.; Fichtner W.; Stricker, A. PARDISO: a high-performance serial and parallel sparse linear solver in semiconductor device simulation. Future Generation Computer Systems, v.18, p.69-78, 2001. https://doi.org/10.1016/S0167-739X(00)00076-5

Serna-Saldívar, S. R. O. Cereal grains: properties, processing, and nutritional attributes. 1.ed. Boca Raton: CRC press, 2010. 752p.

Silva, M. V. A.; Martins, M. A.; Faroni, L. R. A.; Bustos-Vanegas, J. D.; Sousa, A. H.; CFD modelling of diffusive-reactive transport of ozone gas in rice grains, Biosystems Engineering, v.179, p.49-58, 2019. https://doi.org/10.1016/j.biosystemseng.2018.12.010

Silva, M. V. A.; Faroni, L. R. A.; Martins, M. A.; Sousa, A. H.; Bustos-Vanegas, J. D. CFD simulation of ozone gas flow for controlling *Sitophilus zeamais* in rice grains, Journal of Stored Products Research, v.88, e101675, 2020. https://doi.org/10.1016/j.jspr.2020.101675

SNAR - Serviço Nacional de Aprendizagem Rural. Grãos: armazenamento de milho, soja, feijão e café. Brasília: Serviço Nacional de Aprendizagem Rural, 2018. 10p.